Glucose-Responsive Microgels Integrated with Enzyme Nanocapsules for Closed-Loop Insulin Delivery

Zhen Gu,[†,‡,§,∥,#] Tram T. Dang,[†,‡,§] Minglin Ma,[†,‡,§] Benjamin C. Tang,[†,‡,§] Hao Cheng,[†,‡] Shan Jiang,[†,‡] Yizhou Dong,[†,‡,§] Yunlong Zhang,[†,‡,§] and Daniel G. Anderson[†,‡,§,⊥,*]

[†]Department of Chemical Engineering, Massachusetts Institute of Technology, 77 Massachusetts Avenue, Cambridge, Massachusetts 02139, United States, [‡]David H. Koch Institute for Integrative Cancer Research, Massachusetts Institute of Technology, 77 Massachusetts Avenue, Cambridge, Massachusetts 02139, United States, [§]Department of Anesthesiology, Children's Hospital Boston, 300 Longwood Avenue, Boston, Massachusetts 02115, United States, [⊥]Division of Health Science and Technology, Massachusetts Institute of Technology, Cambridge, Massachusetts 02139, United States, [∥]Joint Department of Biomedical Engineering, University of North Carolina at Chapel Hill and North Carolina State University, North Carolina 27695, United States, and [#]Molecular Pharmaceutics Division, Eshelman School of Pharmacy, University of North Carolina at Chapel Hill, Chapel Hill, North Carolina 27599, United States

ABSTRACT A glucose-responsive closed-loop insulin delivery system represents the ideal treatment of type 1 diabetes mellitus. In this study, we develop uniform injectable microgels for controlled glucose-responsive release of insulin. Monodisperse microgels ($256 \pm 18\ \mu$m), consisting of a pH-responsive chitosan matrix, enzyme nanocapsules, and recombinant human insulin, were fabricated through a one-step electrospray procedure. Glucose-specific enzymes were covalently encapsulated into the nanocapsules to improve enzymatic stability by protecting from denaturation and immunogenicity as well as to minimize loss due to diffusion from the matrix. The microgel system swelled when subjected to hyperglycemic conditions, as a result of the enzymatic conversion of glucose into gluconic acid and protonation of the chitosan network. Acting as a self-regulating valve system, microgels were adjusted to release insulin at basal release rates under normoglycemic conditions and at higher rates under hyperglycemic conditions. Finally, we demonstrated that these microgels with enzyme nanocapsules facilitate insulin release and result in a reduction of blood glucose levels in a mouse model of type 1 diabetes.

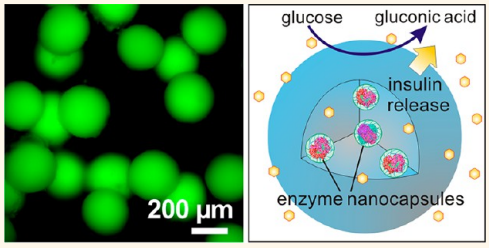

KEYWORDS: drug delivery · diabetes · insulin · glucose-responsive · nanocapsules · microgels

Diabetes mellitus is a metabolic disorder where glucose regulation fails as a result of (1) insufficient production and secretion of insulin from the body due to an autoimmune destruction of pancreatic β-cells (type 1 diabetes) or (2) a combination of impaired insulin resistance and insulin secretion (type 2 diabetes).[1−3] Type 1 and type 2 diabetes affects more than 25.8 million people in the United States, amounting to approximately 8.3% of the population.[4] Multiple subcutaneous injections of insulin and regular monitoring of blood glucose levels are essential for type 1 diabetes patients and some type 2 diabetes patients.[5] However, such self-administration is uncomfortable and painful and requires substantial patient compliance. More importantly, conventional treatment, where glucose sensing and drug therapy are not directly coupled, known as open-loop insulin delivery, does not tightly regulate glucose levels in patients.[6,7] Lack of tight control of blood glucose levels is associated with significant patient disease including limb amputation, blindness, kidney failure, and fatal hypoglycemia.[8]

An artificial pancreas-like closed-loop insulin delivery system that continuously and intelligently releases insulin in response to changing blood glucose levels can improve the quality of life for diabetes patients.[9−12] One strategy to achieve a closed-loop system is to integrate a glucose-monitoring moiety and a sensor-triggered insulin-releasing moiety into a single system.[9,11] Semiautomated closed-loop insulin delivery devices have integrated a continuous glucose-monitoring sensor with an external insulin infusion pump.[11] Nevertheless, engineering an implantable device with the combination of continuous glucose-sensing and self-regulating release remains challenging.[11] In addition to electronic devices, chemically controlled closed-loop delivery platforms

* Address correspondence to dgander@mit.edu.

Received for review April 2, 2013 and accepted July 2, 2013.

Published online July 08, 2013
10.1021/nn401617u

have been explored, typically consisting of polymeric hydrogels that swell or shrink to adjust the insulin release rate according to ambient glucose levels.[9,11,13−21] One approach involves glucose oxidase (GOx), a glucose-specific enzyme that catalyzes glucose to gluconic acid.[12] In such systems, GOx is entrapped or immobilized within a pH-sensitive matrix, and glucose level increases lead to a decrease in the microenvironmental pH.[16,22−24] As a result, the pH-sensitive matrix changes in volume and the release rate of the loaded insulin increases.[9,11] However, bulk-gel-based systems suffer from slow response rates to changes in glucose concentration, leading to delayed insulin release.[11] Additionally, GOx-containing membranes suffer from low mechanical strength, which in combination with slow response rates can result in unexpected leaking and risk of hypoglycemia.[11] Current GOx-based systems also suffer from enzyme denaturation, insufficient oxygen levels for catalysis, immunogenicity, and low loading capacity.[11]

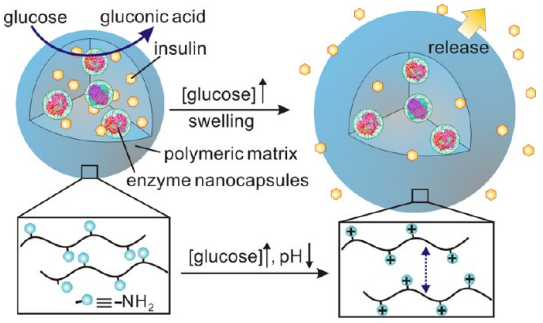

Figure 1. Schematic of microgels encapsulating insulin and enzyme nanocapsules. The encapsulated glucose-specific enzyme catalyzes glucose into gluconic acid. The subsequent protonation of polymer chains with rich amine groups increases the charge in the gel matrix, leading to swelling of the microgels and release of insulin.

Herein, we describe a closed-loop insulin delivery platform composed of injectable microgels, which releases insulin in a glucose-responsive fashion. As shown in Figure 1, each microgel consists of three components: (1) a physically cross-linked pH-responsive polymeric matrix; (2) GOx- and catalase (CAT)-containing enzyme nanocapsules; and (3) human recombinant insulin. The enzyme GOx generates a pH change in response to glucose; CAT is added to regenerate oxygen (O_2) to assist GOx's glucose catalysis and consume undesired hydrogen peroxide (H_2O_2) produced by glucose oxidation, which may be toxic to the body and deactivate GOx. Of note, both enzymes are covalently encapsulated into nanogel-based capsules (Figure 2a) in order to enhance enzymatic stability,[25] avoid denaturation, shield from immunogenicity, and minimize enzyme diffusion from the polymeric matrix. Continuous swelling leads to expansion and dissociation of the polymeric network, which in turn triggers insulin release. Additionally, the acidic environment increases the solubility of insulin, further increasing the insulin release rate. Importantly, this system is reversible, and under normoglycemic

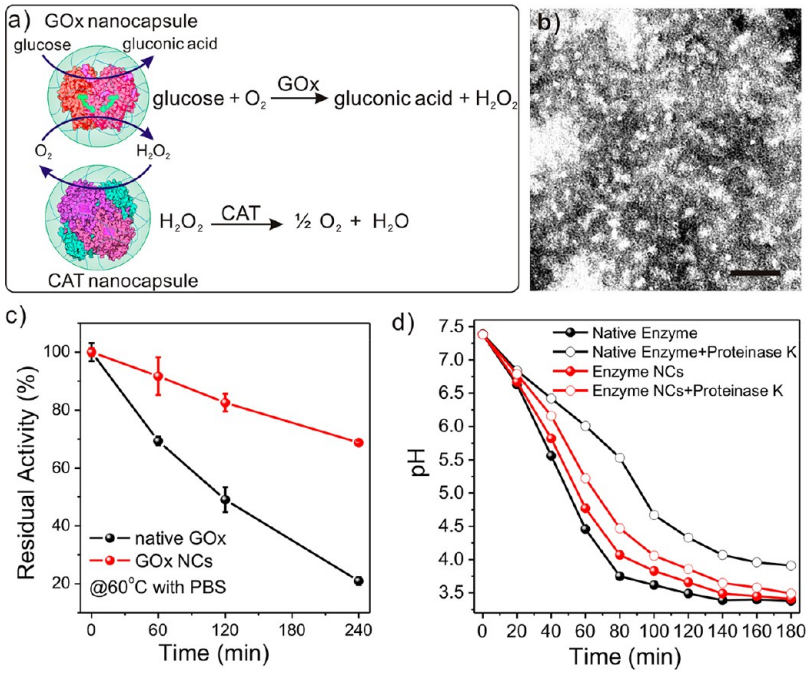

Figure 2. Characterization of enzymatic nanocapsules (NCs). (a) Enzymatic reactions involving glucose oxidase (GOx) and catalase (CAT) nanocapsules. (b) TEM image of a mixture of GOx and CAT nanocapsules. Scale bar: 50 nm. (c) Comparison of enzyme stabilities of native GOx and GOx nanocapsules at 60 °C in PBS buffer. (d) Comparison of catalytic activity of native enzymes (mixture of GOx and CAT, 0.15 mg/mL, weight ratio of GOx to CAT: 4:1) and enzyme nanocapsules incubated with a 400 mg/dL glucose saline solution after incubation with proteinase K (1 mg/mL) at 37 °C for 24 h.

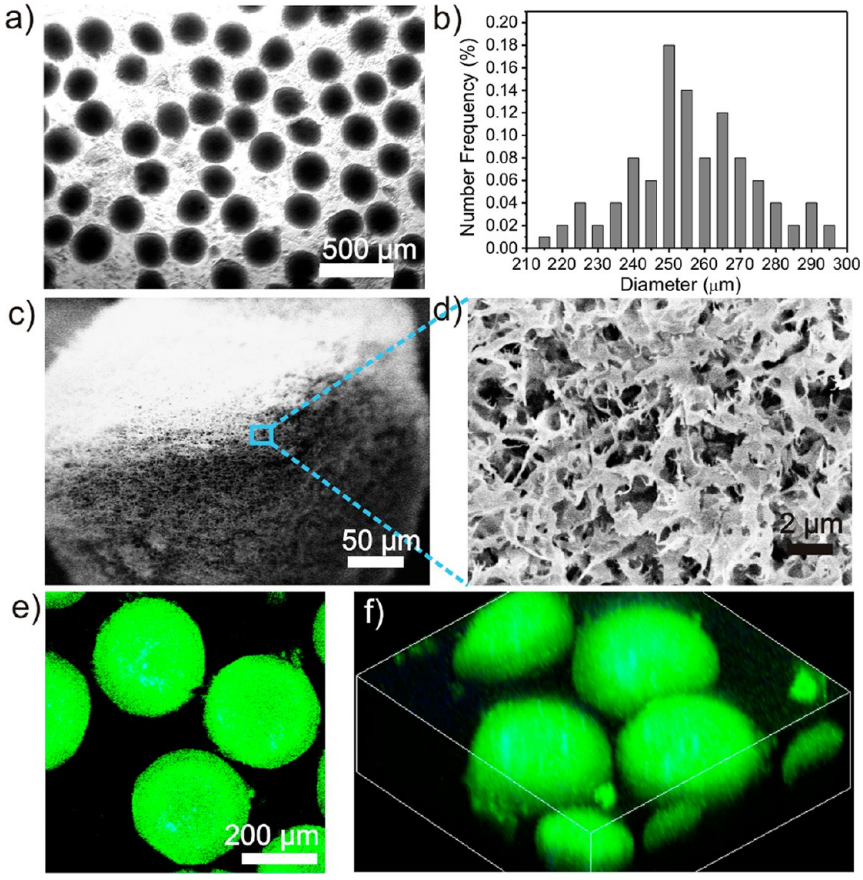

Figure 3. Characterization of microgels encapsulating insulin and enzyme nanocapsules. (a) Optical microscope image of microgels and the statistical distribution of their diameters (b). (c, d) SEM images of insulin-loaded microgels after lyophilization. (e) Laser scanning confocal microscopy image and (f) a 3D reconstructed confocal image of microgels encapsulating FITC conjugated insulin (green) and DyLight 650 conjugated enzymes (blue). Scale bars: (a) 500 μm; (c) 50 μm; (d) 2 μm; (e) 200 μm.

conditions, the microgels shrink and insulin release ceases.

RESULTS AND DISCUSSION

Formation of Microgels with Enzyme Nanocapsules. Chitosan is the basis of the microgel, due to its successful use in medicine, biocompatibility, and ease of protonation (pK_a: 6.2−6.8).[26] In the body, chitosan can be degraded by ubiquitous lysozymes or glycosidases into amino sugars and subsequently cleared from the body.[26] Chitosan-based microgels were prepared using a one-step process with a high-voltage electrospraying system[27] to obtain monodispersed particles. Tripolyphosphate (TPP) was used to cross-link the chitosan matrix through electrostatic interactions to entrap the enzyme-loaded nanocapsules and insulin. A schematic diagram of the experimental setup is shown in Figure S1 (Supporting Information).

Nanogels encapsulated with GOx or CAT were synthesized by a two-step procedure (Supporting Information, Figure S2).[28,29] Briefly, polymerizable vinyl groups were covalently conjugated to the enzyme. Compact nanocapsules were prepared following free radical polymerization in an aqueous solution containing monomers (acrylamide (AAm) and *N*-(3-aminopropyl)methacrylamide (APMAAm)) and cross-linker (*N*,*N*′-methylenebisacrylamide). Enzyme nanocapsules were spherical and uniform in size, with a diameter of ∼12 nm as determined by transmission electron microscopy (TEM) (Figure 2b) and dynamic light scattering (DLS) analysis (Supporting Information, Figure S3). The circular dichroism (CD) spectra (Supporting Information, Figure S4) of the native and the enzyme nanocapsules confirmed that the enzymes retained the secondary structure of native proteins.

Thermal stability of the native and the GOx nanocapsules was compared by incubating at 60 °C. After 4 h, the enzyme nanocapsule retained 70% of its original activity, whereas the native GOx retained only 20% of its original activity, as shown in Figure 2c. The enhanced thermal stability of the enzyme nanocapsules is likely due to covalent attachment to the protective polymer.[25] To further validate the protective properties of the nanocapsules, enzyme nanocapsules and native enzymes were incubated in 1× PBS solution with proteinase K, which degrades exposed proteins. After 24 h at 37 °C, samples were exposed to 400 mg/dL glucose to determine the enzymatic activity of GOx. As shown in

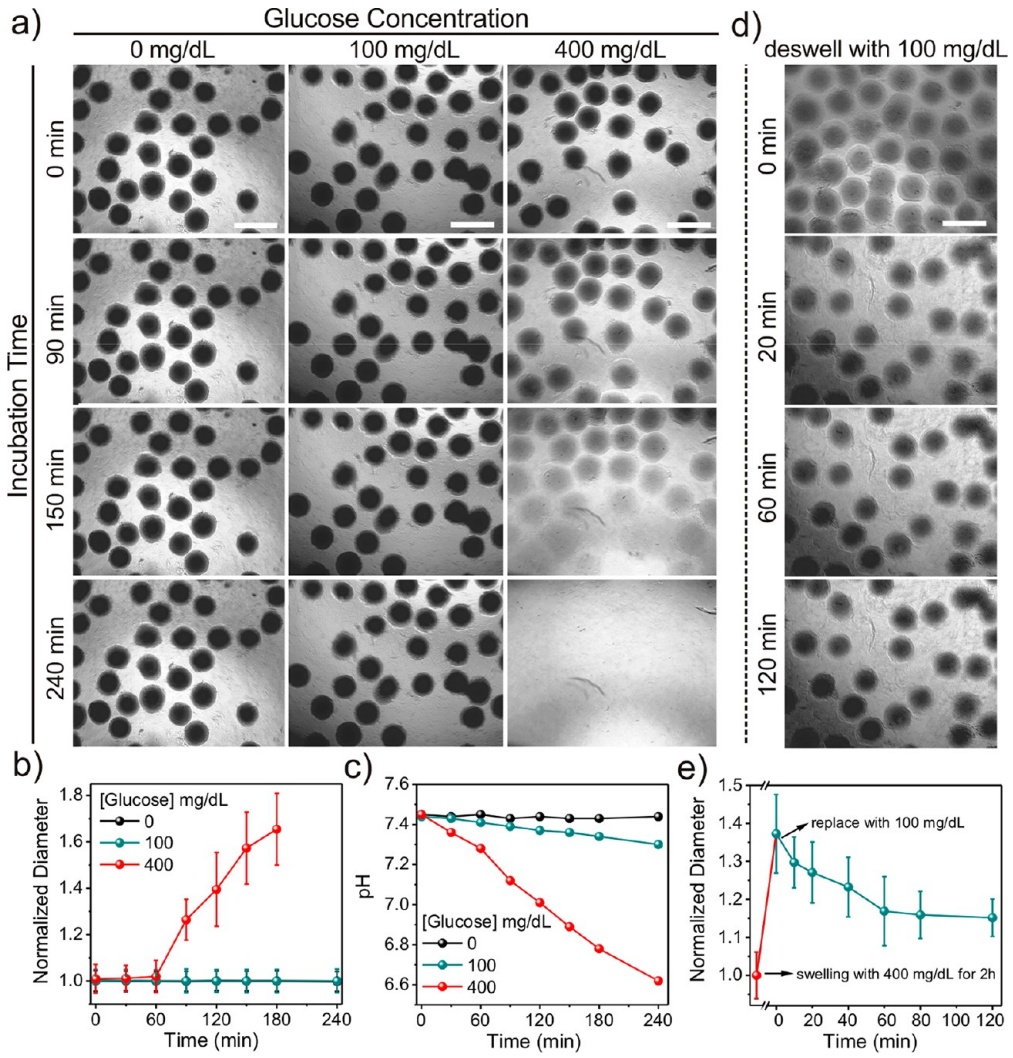

Figure 4. Glucose-responsive properties of self-regulated microgels. (a) Optical microscope images of microgels incubated with 1× PBS solutions at different glucose concentrations (0, 100, and 400 mg/dL) over time at 37 °C. (b) Normalized diameter changes of microgels as a function of time. (c) Relevant pH changes in different incubation solutions. (d) Optical microscope images of a deswelling process over time. Microgels were first incubated with 400 mg/dL glucose for 2 h, which was then replaced with 100 mg/dL glucose for 2 h. (e) Normalized diameter changes of microgels in the deswelling process. Scale bars in (a) and (d) represent 500 μm.

Figure 2d, the rate of pH decrease with native enzymes was reduced after incubation with proteinase K. In contrast, the rate of pH decrease with enzyme nanocapsules was only slightly reduced. Collectively, we can infer that the polymeric shell around the enzymes enhances their stability and protects from loss of activity. Since a higher concentration of CAT would result in less accessible sites on GOx and thus hinder enzymatic oxidation of glucose,[23] the weight ratio of GOx to CAT was optimized and maintained at 4:1 (Supporting Information, Figure S5).[30]

Insulin and enzyme nanocapsules were mixed with sterilized chitosan solution (2% w/v in 1% acetic acid solution at a weight ratio of chitosan/insulin/enzymes of 50/50/4.8). The homogeneous mixture was transferred into a syringe and sprayed at a high voltage (9.0 kV) onto the receiving container with 5% TPP solution for cross-linking. In order to prepare microgels of uniform size, we adjusted the applied voltage and the flow rate of the electrospray to achieve optimal conditions. Using 250 μL/min as a flow rate, spherical and monodispersed gel particles with a diameter of 256 ± 18 μm were obtained (Figure 3a,b). An optimal insulin loading capacity of 44.6 ± 2.8% and encapsulation efficiency of 59.7 ± 3.4% (Supporting Information) were achieved. Scanning electron microscope (SEM) images in Figure 3c,d revealed the porous structure of particles after lyophilization. Laser scanning confocal microscopy images in Figure 3e,f verified that encapsulated fluorescent dye-stained insulin and nanocapsules were homogeneously distributed inside the microgels. The confocal images indicate that insulin is stably encapsulated within the matrix of particles with negligible diffusion, as there was a clear demarcation between the microparticles and the background. This observation can be attributed to the strong electrostatic and van der Waals interactions between insulin and chitosan chains.

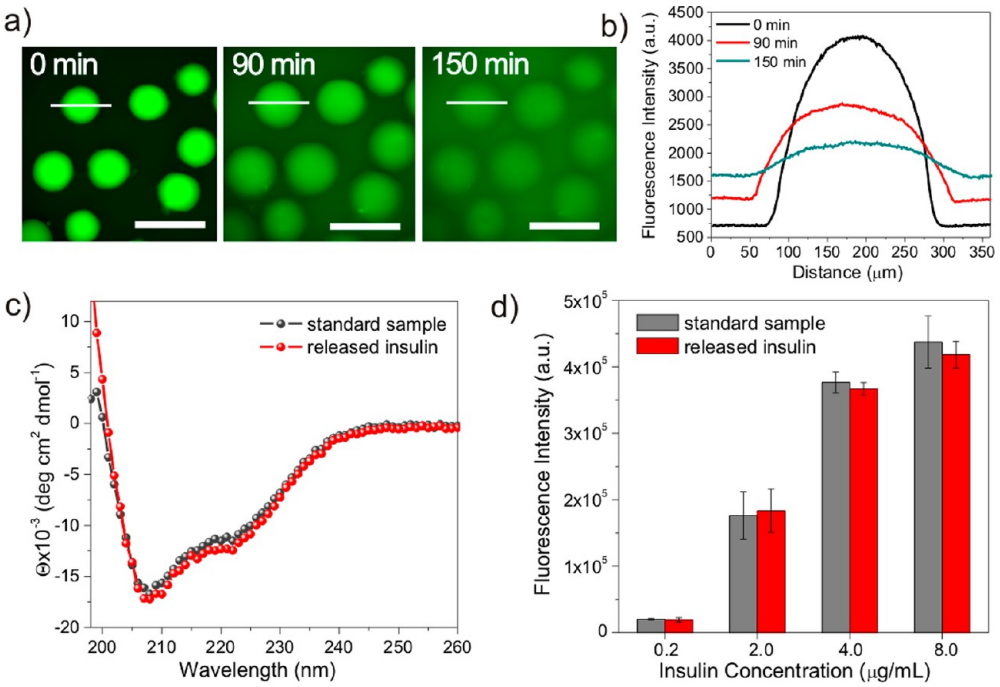

Figure 5. Glucose-responsive insulin release from microgels. (a) Release of FITC-stained insulin from microgels incubated in 400 mg/dL glucose PBS solution over time at 37 °C. (b) Fluorescence intensity profiles of an individual microgel (the one with a white line in a)) as a function of incubation time. (c) CD spectra of standard insulin solution and insulin released from microgels. (d) Insulin activity assays on serial dilutions of standard insulin and insulin released from microgels by AKT phosphorylation following stimulation of the insulin receptor. Scale bar in (a) represents 400 μm.

Validation of Glucose-Responsive Characteristics. To determine glucose responsiveness, microgels were incubated with 1× PBS solutions containing different glucose concentrations, including a hyperglycemic level of 400 mg/dL, a normoglycemic level of 100 mg/dL, and a control level of 0 mg/dL. As shown in Figure 4a, microgels incubated at the hyperglycemic level steadily swelled over time. Within 3 h, the particles exhibited a 1.7-fold change in diameter, corresponding to a 5-fold volume change. In addition, the conversion of glucose to gluconic acid through enzyme nanocapsules resulted in a decrease of solution pH from 7.4 to 6.6, suggesting that the protonation of primary amines of chitosan leads to the swelling of the microgels. After 4 h, the microgels were fully dissociated and the solution became transparent (Figure 4a). In contrast, microgels treated with saline or normal glucose solution did not display noticeable swelling within 4 h, which was associated with only a slight decrease in pH. We also incubated microgels in 400 mg/dL glucose solution for 2 h followed by 100 mg/dL glucose solution. As shown in Figure 4d,e, swollen microgels steadily shrank over time. We hypothesize that deswelling of microgels was driven by the dissociation of hydrogen ions from the chitosan when exposed to a neutral pH solution. Microgels cannot completely revert to the original state, in part due to disassembly of some of the polymeric chains and polyanions into the solution during the swelling process.

We next assessed the insulin release kinetics in response to the glucose level changes. To demonstrate

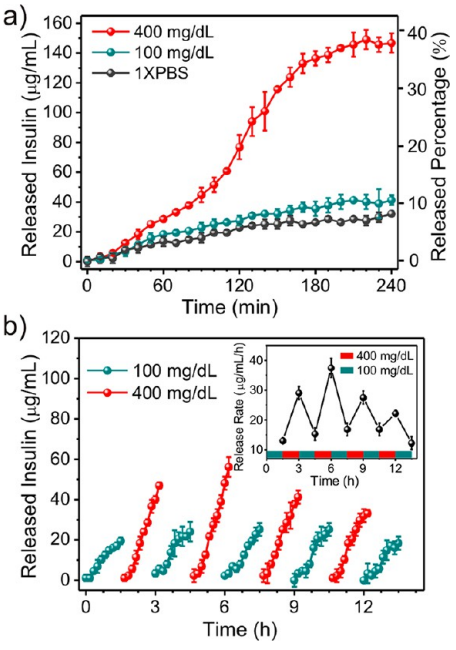

Figure 6. Quantitative examination of glucose-responsive insulin release. (a) *In vitro* release kinetics of insulin from the microgels in 1× PBS solutions with different glucose concentrations: 0, 100, and 400 mg/dL at 37 °C. (b) Self-regulated profile of microgels presenting the rate of insulin release as a function of glucose concentration. Data points represent mean ± SD (n = 3).

temporal release of insulin from the microgel, microgels encapsulating FITC-conjugated insulin were incubated in a 400 mg/dL glucose solution at 37 °C for

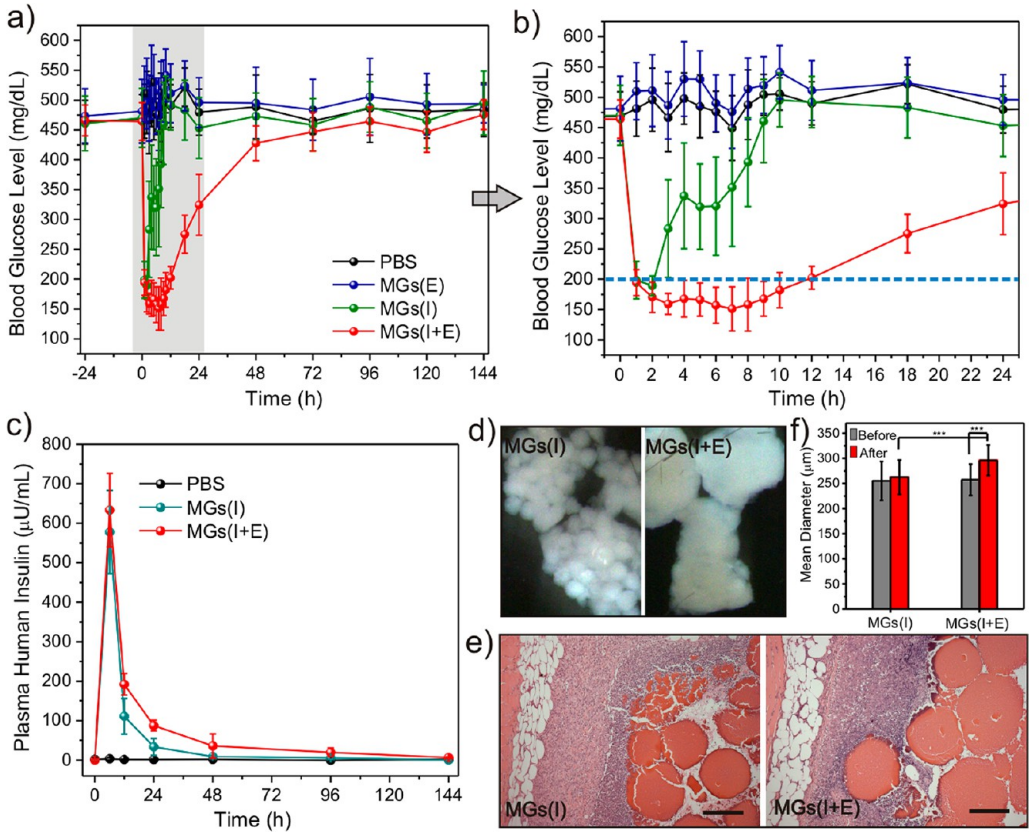

Figure 7. ***In vivo*** **studies of microgels for the treatment of type 1 diabetes. (a) Blood glucose levels in STZ-induced C57B6 diabetic mice after subcutaneous injection with 1× PBS, microgels encapsulating insulin and enzymes (MGs(E+I)), microgels encapsulating insulin only (MGs(I)), microgels encapsulating enzymes only (MGs(E)). (b) Blood glucose levels of each animal group within 24 h after administration, extracted from the shaded part of (a). (c) Plasma human insulin levels of mice treated with 1× PBS, MGs(E+I), and MGs(I) over the administration time. (d) Pictures of microgels withdrawn from diabetic mice 3 days after administration. (e) Representative H&E staining of mice dermal tissues containing MGs(E+I) and MGs(I). (f) Changes of mean diameters of MGs(E+I) and MGs(I) 3 days after administration. Data points in (a)−(c) represent mean ± SD (n = 6 for the group administrated with MG(E), MG(I), and MG(E+I); n = 4 for the group administrated with PBS); data points in (f) represent mean ± SD (n = 50) and *** represents $p < 0.001$ by Student's t-test. Scale bar in (e) represents 200 μm.**

150 min. Fluorescence images of microgels were recorded and analyzed over time. As shown in Figure 5a,b, as the microgel sizes increased, the fluorescence intensity of the microgel gradually decreased, and the fluorescence intensity of the solution increased, indicating that the encapsulated insulin steadily released from the chitosan matrix into the exterior solution. Furthermore, the CD spectrum of the released insulin from microgels matched that of free insulin (Figure 5c). To confirm the bioactivity of the released insulin, we evaluated the activity of insulin released from the microgels using a cell-based assay that quantifies AKT phosphorylation, which follows the stimulation of insulin receptor by a native insulin. Released insulin retained bioactivity comparable to standard samples at the same concentrations (Figure 5d). The enzymatic activity of GOx nanocapsules was maintained in the microgel matrix during expansion when compared with native GOx (Supporting Information, Figure S5c).

To further examine the release from microgels in response to glucose level changes, insulin release studies were performed. We demonstrated that microgels release insulin at hyperglycemic glucose levels (Figure 6a). In contrast, a much slower release rate was obtained when the microgels were exposed to the basal glucose level and control solutions. These results are consistent with the observed swelling response (Figure 4a,b). Importantly, the insulin release profile of microgels presents a pulsatile pattern exposed to an alternating glucose concentration between normal and hyperglycemic levels every 1.5 h for several cycles. Microgels responded to changes in glucose levels with a 2.5-fold increase in the insulin release rate when the glucose concentrations were elevated to hyperglycemic levels (Figure 6b). Interestingly, the release rates at high hyperglycemic level reached a maximum point and then gradually decreased. The "acceleration period" was accounted for by incomplete reversibility between swelling and deswelling, while the "deceleration period" was due to the depletion of insulin in the dissociated microgels. Additionally, we observed that microgels integrated with enzyme nanocapsules showed more robust self-regulating capability compared to those with native enzymes (Supporting Information, Figure S7),

which can be ascribed to less diffusion of catalytic elements from microgels with enzyme nanocapsules.

***In Vivo* Studies of Microgels.** To evaluate the *in vivo* activity of microgels in type 1 diabetes, streptozotocin (STZ)-induced diabetic mice[31] were divided into four groups and subcutaneously injected with microgels containing human recombinant insulin with enzyme nanocapsules (MGs(I+E)), microgels encapsulating insulin only (MGs(I)), or enzyme nanocapsules only (MGs(E)), and control (1× PBS) solution. The blood glucose levels (BGLs) of each animal group were closely monitored after administration and continuously recorded for 6 days. As shown in Figure 7a,b, BGLs of mice injected with MGs(I+E) or MGs(I) (insulin dose: 40 mg/kg) quickly declined to a normoglycemic state (<200 mg/dL) within 2 h. We attributed this to an initial burst release of dissolved insulin in the injection solution and adsorbed insulin on the surface of microgels. The BGLs of mice with MGs(I+E) were then maintained in the normoglycemic range for up to 12 h and gradually increased afterward. In the absence of the enzyme nanocapsules, the BGLs of mice with MGs(I) steadily increased back to a hyperglycemic state 2 h after injection. Correspondingly, mice treated with MGs(I+E) presented a consistently higher plasma insulin level for at least 96 h than those treated with MGs(I), as quantified by ELISA (Figure 7c). Moreover, similar to the PBS control group, the group treated with MGs(E) did not display a noticeable decline in BGLs, suggesting the catalytic conversion of glucose did not considerably affect BGLs.

Microgels were retrieved from mice 3 days after administration to assess for any toxicity. Microgels with insulin only had a clear circular profile and can be distinguished individually (Figure 7d). In contrast, particles containing enzymes were closely adhered to each other with a bulk gel-like morphology. Further histological investigation of tissues containing injected microgels after 3 days indicated that chitosan microgels induced acute inflammation (Figure 7e). However, chitosan is used medically (Supporting Information, Figure S8) and is enzymatically degradable. The microgels completely degraded 4−6 weeks later, and no fibrotic encapsulation was observed (Supporting Information, Figure S9). We also observed that MGs(I+E) had a significant increase in the mean diameter after implantation, compared with MGs(I) (Figure 7f). This is consistent with swelling induced by enzymatic reactions as observed *in vitro*. This also explains the substantial release of insulin and prolonged maintenance of a normoglycemic state for the system associated with enzymes. Interestingly we note that swelling is reduced when compared to the *in vitro* studies, presumably due to tissue restrictions or buffering in the body.

CONCLUSION

In summary, we have developed enzymatic nanocapsule-containing microgels for glucose-responsive delivery of insulin. The enzymatic conversion of glucose into gluconic acid in the noncovalent cross-linked polymeric matrix reduces the microenvironmental pH, resulting in swelling and dissociation of the microgels, increasing the release rate of insulin. The *in vivo* studies demonstrated that incorporation of enzyme into microgels facilitated the release of insulin and control of blood glucose levels. Further development will be necessary to optimize the glucose response sensitivity and sustain long-term release to achieve dynamic regulation of blood glucose levels under *in vivo* conditions. With the benefits of uniform accessibility, enhanced enzymatic stability, and stimuli controllable capability, we believe this approach has potential for the generation of a glucose-responsive insulin delivery system. We further believe that this platform may be extended to allow co-delivery of other therapeutic agents, including therapeutic proteins and peptides or small molecular anti-inflammation drugs.

METHODS

Materials. All chemicals were purchased from Sigma-Aldrich unless otherwise specified and were used as received. Human recombinant insulin (Zn salt, 27.5 IU/mg) was purchased from Invitrogen. The deionized water was prepared by a Millipore NanoPure purification system (resistivity higher than 18.2 MΩ·cm^{-1}).

Preparation and Characterization of Enzyme Nanocapsules. Single-enzyme-containing nanocapsules were prepared according to our previously reported procedure with modifications.[28,29] Briefly, a volume of 12 mg of GOx or CAT in 4.0 mL of pH 8.5, 50 mM sodium carbonate buffer was reacted with 6 mg of *N*-acryloxysuccinimide in 40 μL of dimethyl sulfoxide (DMSO) for 2 h at room temperature. Buffer exchange with 1× PBS was then carried out three times (Amicon Ultra-15 50 K devices, Millipore Corp.). The degree of modification was 23 vinyl groups per GOx or 32 vinyl groups per CAT, measured using 2,4,6-trinitrobenzene sulfonic acid (Thermo Fisher Scientific Inc.). Modified enzyme was diluted to 1 mg/mL with 10 mM pH 8.5 sodium bicarbonate buffer. Then 40 μL of acrylamide (AAm) monomer, prepared in a 200 mg/mL aqueous solution, was added to 6 mL of protein solution with stirring for 10 min at 4 °C. Subsequently, the other monomer, *N*-(3-aminopropyl)-methacrylamide (APMAAm), was added. Afterward, cross-linker *N*,*N*′-methylenebisacrylamide was added. The molar ratio of AAm/APMAAm/cross-linker was adjusted to 8/4/1. The polymerization was immediately initiated by adding 4 mg of ammonium persulfate dissolved in 40 μL of deoxygenated and deionized water and 4 μL of *N*,*N*,*N*′,*N*′-tetramethylethylenediamine. The polymerization was allowed to proceed for 90 min in a nitrogen atmosphere at room temperature. Finally, buffer exchange with 1× PBS was performed to remove unreacted monomers and initiators. The yield of the enzyme nanocapsules was higher than 95%. The unmodified enzymes were removed using size-exclusion chromatography. The protein content in nanocapsules was determined by the bicinchoninic acid (BCA) colorimetric protein assay. Briefly, a tertrate buffer (pH 11.25) containing 25 mM BCA, 3.2 mM $CuSO_4$, and appropriately diluted protein/NCs was incubated at 60 °C for 30 min. After the solution was cooled to room temperature, absorbance readings at 562 nm were determined with a UV−vis spectrometer (Thermo Scientific GENESYS 20).

BSA solutions with known concentrations were used as standards. The enzymatic activity of native GOx and GOx nanocapsules was tested by the Amplex Red glucose/glucose oxidase assay kit (Invitrogen).

Preparation of Microgels. An aqueous solution of chitosan (2% w/v) was prepared by dissolving sterilized chitosan powder (molecular weight: ~200 kDa) in 1% acetic acid solution. The obtained solution was centrifuged at 10 000 rpm to remove undissolved impurities. Insulin and enzyme nanocapsules were added and thoroughly mixed with the chitosan solution. The weight ratio of chitosan/insulin/enzymes was 50/50/4.8. The homogeneous mixture was transferred into a 5 mL syringe with an attached blunt tip, 30 gauge metal needle. The syringe was placed in an electrospray system equipped with a syringe pump. The positive electrode of the electrospray system was connected to the needle, and the negative electrode was connected to a sterile metal receiving container with 50 mL of 5% TPP. The solution was sprayed at high voltage to the receiving container with gentle agitation. The collected particles were washed with 1× PBS twice and concentrated by centrifugation at 2000 rpm. The microparticles were stored at 4 °C with a final density of ~2000 particles/mL (insulin content: ~3.2 mg/mL). The loading capacity (LC) and encapsulation efficiency (EE) of microgels were calculated as LC = $(A - B)/C$ and EE = $(A - B)/A$, where A was the expected encapsulated amount of insulin or enzyme, B was the free amount of insulin or enzyme in the collection solution, and C was the total weight of particles.

***In Vitro* Insulin Release from Microgels.** To determine glucose response capability of microgels, microgels (insulin content: ~0.2 mg) were collected by spinning down to pellets at 3000 rpm for 30 s and incubated with 0.5 mL of 1× PBS solutions with different glucose levels (0, 100, and 400 mg/dL) in a 48-well plate, which was left on a heating stage fixed at 37 °C. Optical or fluorescence microscopy images of microgels incubated in different solutions were separately recorded over time. For plotting the accumulated release profile, microgels were similarly incubated with solutions at different glucose levels at 37 °C. The insulin content was measured using a Coomassie Plus protein assay. The absorbance of the well was detected at 595 nm, and the concentration was interpolated from an insulin standard curve and a calibration curve made using microgels encapsulated with enzyme nanocapsules only. To assess the self-regulated release profile, microgels were first incubated in 100 mg dL^{-1} glucose for 1.5 h at 37 °C. The sample was then centrifuged at 3000 rpm for 30 s, and all of the supernatant was recovered. Next, the sample was incubated in 400 mg dL^{-1} glucose for another 1.5 h. This cycle was repeated for subsequent alternating cycles. Similarly, insulin concentration was determined using the Coomassie Plus protein assay. The insulin release rates were determined by the slope of the curves. Bioactivity of released insulin from microgels was tested by the stimulation of an insulin receptor based AKT phosphorylation assay. CHO-M1 cells (ATCC) were seeded at 25 000 cells/well in a 96-well plate and allowed to grow for 24 h before serum-starving overnight. Serum-starved cells were treated with insulin samples with different concentrations for 10 min. Cells were then lysed, and AKT phosphorylation at S473 was assayed according to the manufacturer's protocol (AlphaScreen, Perkin-Elmer).

***In Vivo* Studies Using STZ-Induced Diabetic Mice.** The efficacy of the insulin-loaded microgels for diabetes treatment was evaluated *in vivo* using STZ-induced adult diabetic mice (male C57B6, Jackson Lab, USA). Mice were cared for under supervision of MIT's Division of Comparative Medicine and in compliance with NIT's Principles of Laboratory Animal Care. The blood glucose levels of mice were continuously tested for 2 days before administration by collecting blood (~3 μL) from the tail vein and measuring using the Clarity GL2Plus glucose monitor (VWR, USA). Six diabetic mice were selected for each group administered with microgels loaded with human recombinant insulin and enzyme nanocapsules, microgels loaded with insulin only, or microgels with enzyme nanocapsule only. Four diabetic mice were selected for the group administered with PBS solution. A 250 μL amount of microgel solutions or PBS solution was injected using a 1 cm^3 syringe with a 19-gauge needle into the subcutaneous dorsum of mice (insulin dose: 40 mg/kg) that had been anesthetized with 1% isoflurane. The glucose level of each mouse was monitored over time. To measure *in vivo* insulin concentration, blood samples (~25 μL) were drawn from the tail vein of mice and collected into Sarstedt serum gel microtubes. Serum samples (5 μL) were stored frozen at −20 °C until assayed. Plasma insulin concentrations were determined using the human insulin ELISA kit (Calbiotech, USA).

Conflict of Interest: The authors declare no competing financial interest.

Acknowledgment. This work was supported by grant 09PG-T1D027 from the Leona M. and Harry B. Helmsley Charitable Trust Foundation and the Juvenile Diabetes Research Foundation International (JDRF). The authors thank Dr. Q. Wang, Ms. A. Thai, Mr. J. Slosberg, and Ms. J. Di for helpful discussions and assistance with animal studies. The authors would also thank the Tayebati Family Foundation for their generous support of this work.

Supporting Information Available: Experimental details for preparation and characterization of microgels, *in vitro* and *in vivo* studies. This material is available free of charge *via* the Internet at http://pubs.acs.org.

REFERENCES AND NOTES

1. Pickup, J. C.; Zhi, Z. L.; Khan, F.; Saxl, T.; Birch, D. J. Nanomedicine and Its Potential in Diabetes Research and Practice. *Diabetes Metab. Res. Rev.* **2008**, *24*, 604–610.
2. Stumvoll, M.; Goldstein, B. J.; van Haeften, T. W. Type 2 Diabetes: Principles of Pathogenesis and Therapy. *Lancet* **2005**, *365*, 1333–1346.
3. Kahn, C. R. Banting Lecture. Insulin Action, Diabetogenes, and the Cause of Type II Diabetes. *Diabetes* **1994**, *43*, 1066–1084.
4. *Diabetes Statistics 2012*; American Diabetes Association, 2012.
5. Owens, D. R.; Zinman, B.; Bolli, G. B. Insulins Today and Beyond. *Lancet* **2001**, *358*, 739–746.
6. Jeandidier, N.; Boivin, S. Current Status and Future Prospects of Parenteral Insulin Regimens, Strategies and Delivery Systems for Diabetes Treatment. *Adv. Drug Delivery Rev.* **1999**, *35*, 179–198.
7. Owens, D. R. New Horizons-Alternative Routes for Insulin Therapy. *Nat. Rev. Drug Discovery* **2002**, *1*, 529–540.
8. The Diabetes Control and Complications Trial Research Group. The Effect of Intensive Treatment of Diabetes on the Development and Progression of Long-Term Complications in Insulin-Dependent Diabetes Mellitus. *N. Engl. J. Med.* **1993**, *329*, 977–986.
9. Bratlie, K. M.; York, R. L.; Invernale, M. A.; Langer, R.; Anderson, D. G. Materials for Diabetes Therapeutics. *Adv. Healthcare Mater.* **2012**, *1*, 267–284.
10. Kumareswaran, K.; Evans, M. L.; Hovorka, R. Artificial Pancreas: An Emerging Approach to Treat Type 1 Diabetes. *Expert Rev. Med. Devices* **2009**, *6*, 401–410.
11. Ravaine, V.; Ancla, C.; Catargi, B. Chemically Controlled Closed-Loop Insulin Delivery. *J. Controlled Release* **2008**, *132*, 2–11.
12. Wu, Q.; Wang, L.; Yu, H. J.; Wang, J. J.; Chen, Z. F. Organization of Glucose-Responsive Systems and Their Properties. *Chem. Rev.* **2011**, *111*, 7855–7875.
13. Podual, K.; Doyle, F. J.; Peppas, N. A. Preparation and Dynamic Response of Cationic Copolymer Hydrogels Containing Glucose Oxidase. *Polymer* **2000**, *41*, 3975–3983.
14. Ishihara, K.; Kobayashi, M.; Ishimaru, N.; Shinohara, I. Glucose-Induced Permeation Control of Insulin through a Complex Membrane Consisting of Immobilized Glucose-Oxidase and a Poly(Amine). *Polym. J.* **1984**, *16*, 625–631.
15. Makino, K.; Mack, E. J.; Okano, T.; Kim, S. W. A Microcapsule Self-Regulating Delivery System for Insulin. *J. Controlled Release* **1990**, *12*, 235–239.
16. Gordijo, C. R.; Koulajian, K.; Shuhendler, A. J.; Bonifacio, L. D.; Huang, H. Y.; Chiang, S.; Ozin, G. A.; Giacca, A.; Wu, X. Y. Nanotechnology-Enabled Closed Loop Insulin Delivery Device: *In Vitro* and *in Vivo* Evaluation of Glucose-Regulated

Insulin Release for Diabetes Control. *Adv. Funct. Mater.* **2011**, *21*, 73–82.
17. Kataoka, K.; Miyazaki, H.; Bunya, M.; Okano, T.; Sakurai, Y. Totally Synthetic Polymer Gels Responding to External Glucose Concentration: Their Preparation and Application to On-Off Regulation of Insulin Release. *J. Am. Chem. Soc.* **1998**, *120*, 12694–12695.
18. Kataoka, K.; Miyazaki, H.; Okano, T.; Sakurai, Y. Sensitive Glucose-Induced Change of the Lower Critical Solution Temperature of Poly[N,N-dimethylacrylamide-co-3-(acrylamido)-phenyl-boronic acid] in Physiological Saline. *Macromolecules* **1994**, *27*, 1061–1062.
19. Wu, W. T.; Mitra, N.; Yan, E. C. Y.; Zhou, S. Q. Multifunctional Hybrid Nanogel for Integration of Optical Glucose Sensing and Self-Regulated Insulin Release at Physiological pH. *ACS Nano* **2010**, *4*, 4831–4839.
20. Matsumoto, A.; Ishii, T.; Nishida, J.; Matsumoto, H.; Kataoka, K.; Miyahara, Y. A Synthetic Approach Toward a Self-Regulated Insulin Delivery System. *Angew. Chem., Int. Ed.* **2012**, *51*, 2124–2128.
21. Kim, H.; Kang, Y. J.; Kang, S.; Kim, K. T. Monosaccharide-Responsive Release of Insulin from Polymersomes of Polyboroxole Block Copolymers at Neutral pH. *J. Am. Chem. Soc.* **2012**, *134*, 4030–4033.
22. Fischel-Ghodsian, F.; Brown, L.; Mathiowitz, E.; Brandenburg, D.; Langer, R. Enzymatically Controlled Drug Delivery. *Proc. Natl. Acad. Sci. U.S.A.* **1988**, *85*, 2403–2406.
23. Traitel, T.; Cohen, Y.; Kost, J. Characterization of Glucose-Sensitive Insulin Release Systems in Simulated *in Vivo* Conditions. *Biomaterials* **2000**, *21*, 1679–1687.
24. Podual, K.; Doyle, F. J.; Peppas, N. A. Glucose-Sensitivity of Glucose Oxidase-Containing Cationic Copolymer Hydrogels Having Poly(ethylene glycol) Grafts. *J. Controlled Release* **2000**, *67*, 9–17.
25. Yan, M.; Ge, J.; Liu, Z.; Ouyang, P. Encapsulation of Single Enzyme in Nanogel with Enhanced Biocatalytic Activity and Stability. *J. Am. Chem. Soc.* **2006**, *128*, 11008–11009.
26. Kumar, M. N.; Muzzarelli, R. A.; Muzzarelli, C.; Sashiwa, H.; Domb, A. J. Chitosan Chemistry and Pharmaceutical Perspectives. *Chem. Rev.* **2004**, *104*, 6017–6084.
27. Chakraborty, S.; Liao, I. C.; Adler, A.; Leong, K. W. Electrohydrodynamics: A Facile Technique to Fabricate Drug Delivery Systems. *Adv. Drug Delivery Rev.* **2009**, *61*, 1043–1054.
28. Yan, M.; Du, J.; Gu, Z.; Liang, M.; Hu, Y.; Zhang, W.; Priceman, S.; Wu, L.; Zhou, Z. H.; Liu, Z. *et al.* A Novel Intracellular Protein Delivery Platform Based on Single-Protein Nanocapsules. *Nat. Nanotechnol.* **2010**, *5*, 48−53.
29. Gu, Z.; Yan, M.; Hu, B.; Joo, K. I.; Biswas, A.; Huang, Y.; Lu, Y.; Wang, P.; Tang, Y. Protein Nanocapsule Weaved with Enzymatically Degradable Polymeric Network. *Nano Lett.* **2009**, *9*, 4533–4538.
30. Gu, Z.; Aimetti, A. A.; Wang, Q.; Dang, T. T.; Zhang, Y.; Veiseh, O.; Cheng, H.; Langer, R. S.; Anderson, D. G. Injectable Nano-Network for Glucose-Mediated Insulin Delivery. *ACS Nano* **2013**, *7*, 4194–4201.
31. Konrad, R. J.; Mikolaenko, I.; Tolar, J. F.; Liu, K.; Kudlow, J. E. The Potential Mechanism of the Diabetogenic Action of Streptozotocin: Inhibition of Pancreatic Beta-Cell *O*-GlcNAc-Elective *N*-acetyl-Beta-*D*-Glucosaminidase. *Biochem. J.* **2001**, *356*, 31–41.